

Algorithms for detecting dependencies and rigid subsystems for CAD[☆]

James Farre^{a,1}, Helena Kleinschmidt^b, Jessica Sidman^{b,2}, Audrey St. John^{b,3},
Stephanie Stark^{b,4}, Louis Theran^{c,5}, Xilin Yu^{b,6}

^a*Department of Mathematics, University of Utah, Salt Lake City, USA*

^b*Mount Holyoke College, South Hadley, MA USA*

^c*Aalto Science Institute and Department of Computer Science
Aalto University, 00076 Aalto, Finland*

Abstract

Geometric constraint systems underly popular Computer Aided Design software. Automated approaches for detecting dependencies in a design are critical for developing robust solvers and providing informative user feedback, and we provide algorithms for two types of dependencies. First, we give a pebble game algorithm for detecting generic dependencies. Then, we focus on identifying the “special positions” of a design in which generically independent constraints become dependent. We present combinatorial algorithms for identifying subgraphs associated to factors of a particular polynomial, whose vanishing indicates a special position and resulting dependency. Further factoring in the Grassmann-Cayley algebra may allow a geometric interpretation giving conditions (e.g., “these two lines being parallel cause a dependency”) determining the special position.

Keywords: sparsity matroid, pebble game algorithm, cad constraints

[☆]An extended abstract of this article appeared as “Detecting dependencies in geometric constraint systems” in the 10th International Workshop on Automated Deduction in Geometry (ADG 2014), Coimbra, Portugal, 2014.

Email addresses: jamesrfarre@gmail.com (James Farre), klein23h@mholyoke.edu (Helena Kleinschmidt), jsidman@mholyoke.edu (Jessica Sidman), astjohn@mholyoke.edu (Audrey St. John), stark23s@mholyoke.edu (Stephanie Stark), louis.theran@aalto.fi (Louis Theran), yu25x@mholyoke.edu (Xilin Yu)

¹Partially supported by NSF DMS-0849637.

²Partially supported by NSF DMS-0849637 and the Hutchcroft fund.

³Partially supported by the Clare Boothe Luce Foundation, NSF DMS-0849637, NSF IIS-1253146 and the Hutchcroft fund.

⁴Partially supported by the Mount Holyoke College Lynk Program.

⁵Partially supported by the European Research Council under the European Union’s Seventh Framework Programme (FP7/2007-2013) / ERC grant agreement no 247029-SDModels, Academy of Finland (AKA) project COALESCE, and the Hutchcroft fund.

⁶Partially supported by NSF IIS-1253146, an Aalto Science Institute (AScI) Internship, and the Mount Holyoke College Lynk Program.

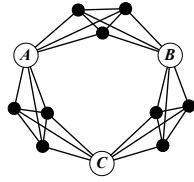
1. Introduction

Constraint-based Computer Aided Design (CAD) software, such as the popular SolidWorks program, allows engineers to create designs using intuitive geometric constraints. When a user adds a constraint that is *dependent*, the resulting system is *over-constrained*. To provide useful feedback, efficient approaches are required to detect the minimal sub-system containing the dependency. In this paper, we present graph-based algorithms for decomposing the underlying combinatorial structure of a system of CAD constraints. This decomposition allows us to associate polynomials whose vanishing indicates the existence of dependencies to subsets of constraints.

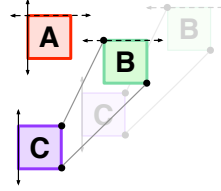
1.1. Motivation

Automated methods for the detection and resolution of dependencies in a CAD system are important for the underlying solver as well as the user. Adding a constraint to a fully defined sub-system with no relative motion among its parts, or *rigid block*, results in a dependency. The rigidity models of 2D *bar-and-joint* and d -dimensional *body-and-bar* are well-known for having combinatorial characterizations of *generically rigid* frameworks (a *bar* imposes a distance constraint between a pair of points). However, a combinatorial characterization for 3D bar-and-joint generic rigidity remains a conspicuously open problem. One property highlighted as a potential barrier is the existence of *contextually rigid components* [1], which do not appear in 2D bar-and-joint or d -dimensional body-and-bar frameworks. A rigid component is a vertex-maximal rigid block, and a *contextually rigid component* is one that is not rigid as an induced framework. Figure 1(a) depicts the well-known 3D bar-and-joint “triple banana” example, in which each “banana” (a K_5 without an edge) is a rigid component; there is a fourth contextually rigid component formed by $\{A, B, C\}$. Contextually rigid components may arise in CAD systems *even in the plane* where generic rigidity is understood combinatorially in all dimensions [2]. We give an example of this phenomenon in Figure 1(b) which depicts a system of 3 rigid bodies in the plane; bodies B and C form a rigid component, but this subsystem is flexible as an induced framework.

In Figure 2 we change the parallel constraints for the framework in Figure 1(b) to line-line coincidence constraints to produce a rigid framework that demonstrates a related problem in detecting dependencies for a system that is in a *special position*. SolidWorks correctly identifies the system in Figure 2 as “Fully Defined,” and the framework satisfies the *genericity* assumptions of the associated *body-and-cad* rigidity model; adding any constraint will result in a dependency. However, simply changing the attachment point of one bar results in a special (*non-generic*) position that is *flexible*, and SolidWorks correctly identifies it as “Under Defined”; see Figure 3(a). The constraint is now dependent, but its consistency with the rest of the system permits a motion. Embedding the same special position in the 3D Assembly environment highlights the difficulty that SolidWorks appears to have; even though the design should permit the same motion, it is now detected as “Over Defined” (see Figure 3(b)). The



(a) The well-known “triple banana” 3D bar-and-joint framework spanning 12 joints is flexible as each “banana” can rotate. This framework has a contextually rigid block $\{A, B, C\}$ that is flexible as an induced framework, since there are no constraints among A, B and C .



(b) A flexible 2D body-and-cad framework consisting of 3 bodies with the following 4 constraints: dashed lines on A and B must be parallel; solid lines on A and C must be parallel; two bars between bodies B and C fix the distance between pairs of points. The contextually rigid block $\{B, C\}$ is flexible as an induced framework.

Figure 1: Contextually rigid blocks highlight behavior that does not appear in 2D bar-and-joint and d -dimensional body-and-bar rigidity models.

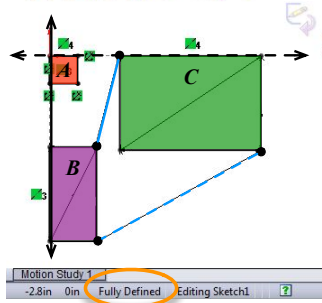
underlying combinatorics of the rigid and flexible systems are the same, and it is the *geometry of the constraints (the two bars are parallel) that leads to the special position and associated dependency*.

1.2. Related work

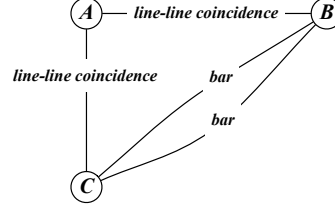
In bar-and-joint and body-and-bar rigidity theory, constraints are specified by fixing the distance between pairs of points and can be represented by quadratic equations. Many other geometric constraints can also be represented by polynomial equations, and it is possible to use algebraic methods to study systems of geometric constraints and their consequences. See [3] for an introduction to automated theorem proving based on Wu’s method. More recent work of [4] uses ideas from algebraic geometry to find special positions of the Stewart-Gough platform, and generalized Stewart-Gough platforms (with angle constraints allowed) were studied in [5].

However, working algebraically with polynomials is limited because it is computationally intensive. Hence, much work in rigidity theory instead focuses on *infinitesimal rigidity*. A structure is *generically minimally infinitesimally rigid* if a certain *rigidity matrix* has maximal rank for some realization of the underlying graph. As a matrix drops rank on a closed set, *almost every* framework with the same combinatorics is infinitesimally rigid (and therefore rigid). Thus, one may detect generic dependencies numerically, by picking random realizations. This is the approach taken by the “witness method” of [6]. The drawback of numerical methods is that fast, stable, algorithms, such as SVD, do not identify the support of a minimal dependency while those based on Gaussian elimination are not stable. (This can be overcome by using finite fields and the Schwartz Lemma, as discussed in [7].)

Generic rigidity of a system is defined via the rank of the rigidity matrix, which we analyze by studying a polynomial called the *pure condition*. The pure



(a) SolidWorks' 2D Sketch environment identifies the **rigid generic** embedding as “Fully Defined.”



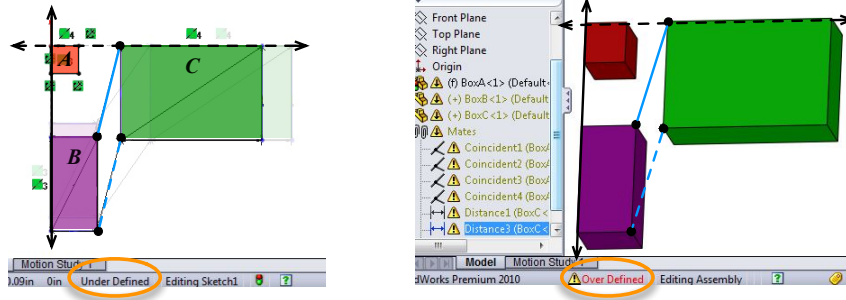
(b) The underlying combinatorics of the framework is captured by a multigraph with a vertex for each body and labeled edge for each constraint.

Figure 2: A generically rigid 2D body-and-cad framework consisting of 3 bodies with the following 4 constraints: a line-line coincidence along the horizontal dashed line for A and B ; a line-line coincidence along the vertical solid line for A and C ; two bars between bodies B and C .

condition of a body-and-bar framework was introduced by White and Whiteley [8], who showed how to interpret the irreducible factors combinatorially and how to describe some special positions using synthetic geometry via the Grassmann-Cayley algebra.

For certain structural models more robust combinatorial characterizations of generic rigidity are known. Particularly relevant here are results for geometric constraints arising in CAD: 2D point-line frameworks [9] and body-and-cad frameworks in 2D and 3D (omitting point-point coincidences) [2]. Combinatorial counting conditions arise as necessary conditions for rigidity theory, usually in terms of a family of “sparse matroidal graphs” that are fundamental in generic rigidity theory (see [10, Appendix], which reports work of White and Whiteley). Associated pebble game algorithms can be used to check rigidity and detect components, relying on the matroidal property of [11, 12]. For body-and-bar [13] and 2D bar-and-joint [14] frameworks, the counting conditions are generically sufficient as well. Owen and Jackson show how to adapt Edmonds’ matroid union algorithm to the framework of pebble games for 2D point-line frameworks in [9]. A combinatorial characterization of 3D bar-and-joint rigidity remains an open problem; while the network flow approach of [15] gives a polynomial time algorithm for the related concept of *module-rigidity*, the class of module-rigid graphs does not include rigid *nucleation-free graphs* [1].

In this paper, we will see that by combining combinatorial and algebraic viewpoints, we can extract even more information and analyze *special positions* which are not covered by the combinatorial theorems.



(a) SolidWorks' 2D Sketch environment gives an identification of "Under Defined," but does not reliably allow the user to explore the allowable motion. The faded position was found by suppressing the dependent constraint, then investigating the motion before unsuppressing it.

(b) SolidWorks' 3D Assembly environment gives a different identification of "Over Defined" for the same design embedded in 3D. No motion can be explored without suppressing the dependent constraint.

Figure 3: Commercial CAD software, such as SolidWorks, is unreliable when presented with a *flexible special position*. This system shares the underlying combinatorics of Figure 2, but the placement of one bar (dashed) is changed to be dependent on the other constraints. The (consistent) dependency arises due to the *geometric condition* that the two bars between *B* and *C* are parallel.

1.3. Contributions

We present algorithms for detecting dependencies in CAD systems modeled as body-and-cad frameworks. The first is a pebble game algorithm that can check for *generic dependencies* via the combinatorial property from [2]; when a constraint is determined to be dependent, we additionally detect its *fundamental circuit* (minimal set of constraints involved in the dependency). To adapt the pebble game to our setting, the algorithm needs to partition the edges in a graph and maintain (a, a) -sparsity on one part and (b, b) -sparsity on the other; this may require dynamically adjusting the partitions. To prove that our algorithm is correct, we show that it is implementing Knuth's matroid partitioning algorithm [16].

Additionally, a framework that is generically minimally rigid (thus containing no generic dependencies) may be in a *flexible special position* caused by a non-generic dependency. Since a special position is indicated by the vanishing of a framework's pure condition, we develop algorithms for finding graph minors, which we refer to as *factor graphs*, corresponding to its factors. In the body-and-bar setting of [8], irreducible factor graphs correspond to irreducible isostatic subframeworks. However, in our setting we may have irreducible factors that do not have a natural interpretation as the pure condition of any subframework; in particular, contextually rigid blocks give rise to these.

1.4. Overview

We begin with an introduction to body-and-cad rigidity theory in Section 2. In Section 3, we give two combinatorial descriptions of the pure condition. We explore the correspondence between factors of the pure condition and graph minors in Section 4. Section 5 contains the algorithms for detecting **generic dependencies** and factor graphs, whose vanishing determines when a framework is in a **special position**. We conclude with a case study in Section 6, where we provide geometric conditions for special positions, and conclusions and open questions in Section 7.

2. Background

In this section, we review the fundamentals of body-and-cad rigidity theory; for full technical details, refer to [17] and [2].

2.1. Body-and-cad frameworks

A *body-and-cad framework* consists of n full-dimensional bodies with pairwise *coincidence*, *angular*, or *distance* constraints between them; these *cad* constraints are specified between *geometric elements* which are affine linear spaces (e.g., a point, line or plane in 3D) rigidly affixed to the bodies. The allowed motions of a body-and-cad framework are continuous motions of the bodies that preserve the given constraints. A body-and-cad framework is *rigid* when all of the allowed motions are trivial, i.e., they consist of applying the same rigid-body motion to each of the bodies; otherwise it is *flexible*.

2.1.1. CAD constraints and primitive constraints.

There are 9 different constraint types in 2D and 21 in 3D. Examples of constraints in 2D are: **point-point distance** (a bar), **point-line coincidence**, **point-line distance**, **line-line coincidence**, and **line-line angular**. Each constraint represents *one or more equations* restricting the relative motion of the bodies involved. A constraint can then be further decomposed into *primitive constraints*, which correspond to single equations. Let d be the dimension of the ambient space. Primitive constraints come in two types, which require distinct algebraic treatment: (i) *blind* constraints, that can potentially restrict any of the $\binom{d+1}{2}$ relative degrees of freedom; (ii) *angular* constraints, that restrict only the $\binom{d}{2}$ relative *rotational* degrees of freedom.

2.2. Examples

To give some intuition about body-and-cad rigidity, consider the planar body-and-cad framework in Figure 4⁷. It is composed of two rigid bodies A (the square) and B (the triangle); placing three cad constraints, a **point-line coincidence**, **line-line perpendicular** and **point-line distance**, results in a *generically minimally rigid* (Definition 2.3) framework.

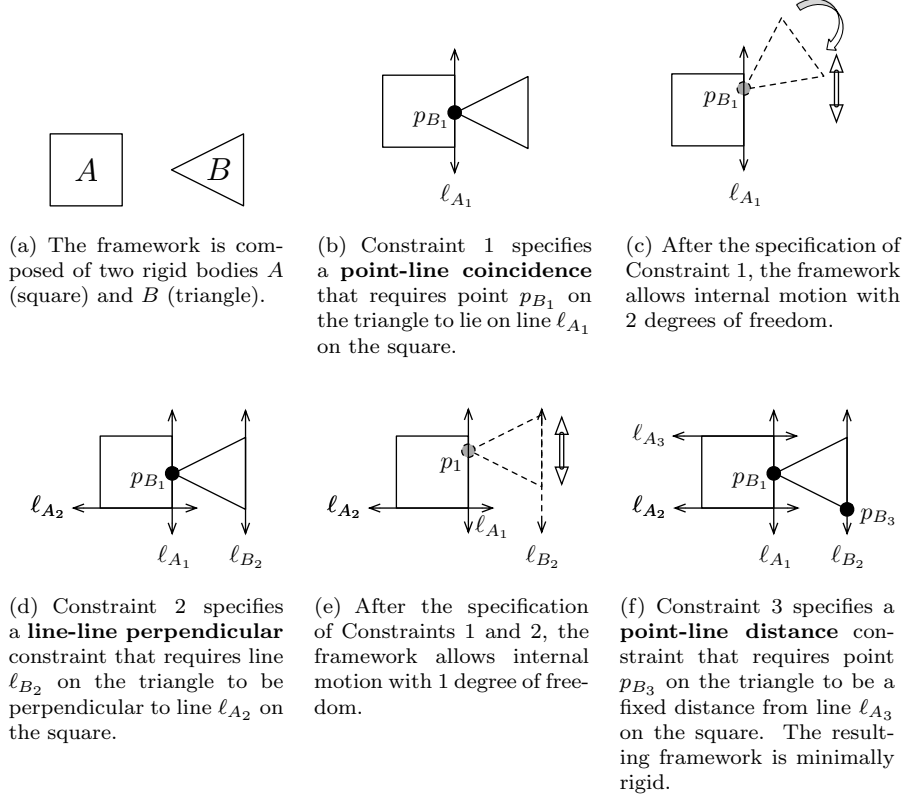


Figure 4: A generically minimally rigid 2D body-and-cad framework.

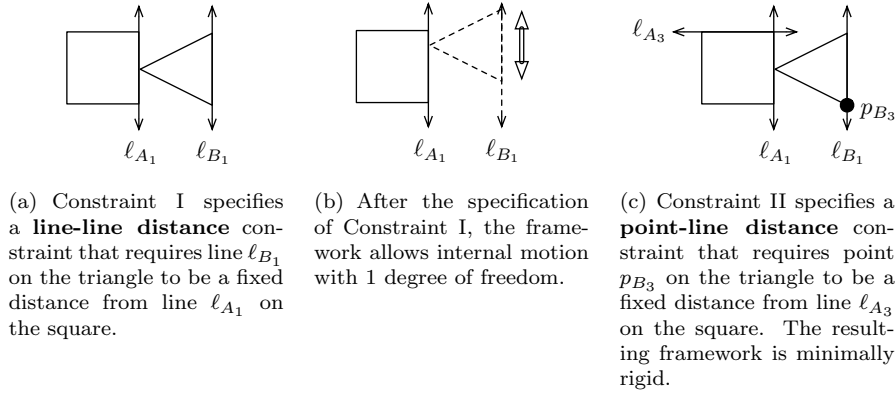
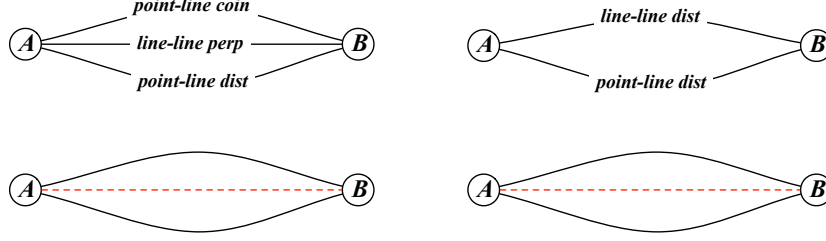


Figure 5: A 2D body-and-cad framework with different geometric constraints but the same rigidity matrix.



(a) The *cad graph* (top) for **Example 1** from Figure 4 has three edges between the vertices for bodies A and B . The **line-line perpendicular** constraint is associated to a primitive angular constraint, so the *primitive cad graph* (bottom) has one red edge.

(b) The *cad graph* (top) for **Example 2** from Figure 5 has two edges between the vertices for bodies A and B . Because the **line-line distance** constraint is associated to two primitive cad constraints (one blind, one angular), the *primitive cad graph* (bottom) has three edges.

Figure 6: Combinatorics of body-and-cad frameworks in Figures 5 and 5: both *cad graphs* (top) are associated to the same *primitive cad graph* (bottom).

Now consider the framework in Figure 5; it is composed of the same two rigid bodies as in Figure 4, but only includes two cad constraints, a **line-line distance** and **point-line distance**. Because Constraint I (**line-line distance**) is equivalent to Constraints 1 and 2 (**point-line coincidence** and **line-line perpendicular**), this system of constraints is equivalent to the figure in Figure 4 and is *generically minimally rigid*.

2.2.1. Combinatorial model.

As discussed above (refer to Figure 5), a single CAD constraint may impose restrictions on multiple degrees of freedom in a framework. Thus, the combinatorial representation for a body-and-cad framework is a *cad graph* which has a vertex for each body and a labeled edge for each cad constraint (refer to the top of Figure 6 for the cad graphs for the examples in Figures 4 and 5).

Associated to each cad graph is a *primitive cad graph*, which is a *bi-colored graph* $G = (V, E = R \sqcup B)$ on vertex set $[n] = \{1, \dots, n\}$ with a vertex for each rigid body, a red edge (in R) for each angular constraint, and a black edge (in B) for each blind constraint. Notice that the primitive cad graphs in Figures 4 and 5 are the same (refer to the bottom of Figure 6).

In the rest of this paper, we will work with primitive cad graphs.

2.2.2. The rigidity matrix and infinitesimal rigidity.

As is standard in the field, we will linearize the geometric constraint equations and consider *infinitesimal rigidity*. Here, the core object of study is a

⁷Note that results in this paper apply in dimension 3 as well.

rigidity matrix (derived in [17]), whose kernel consists of the infinitesimal motions of the framework.

To describe body-and-cad rigidity matrices combinatorially, we use the following concept⁸.

Definition 2.1. For integers a, b , let $k = a + b$. We define an $[a, b]$ -frame $G(\mathbf{p})$ to be a bi-colored graph $G = (V, E = R \sqcup B)$ with $kn - k$ edges, along with a function $\mathbf{p} : E \rightarrow \mathbb{R}^k$. The function \mathbf{p} labels each edge with a k -vector, which is zero in the last b entries if the edge is in R . The generic $[a, b]$ -frame $G(\mathbf{x})$ has formal indeterminates replacing the nonzero coordinates of \mathbf{p} .

We define the rigidity matrix in terms of $[a, b]$ -frames. We first fix some ordering on the edges of G .

Definition 2.2. The rigidity matrix $M(G(\mathbf{p}))$ of an $[a, b]$ -frame $G(\mathbf{p})$ is a matrix that has k columns for each vertex i and one row for each edge of G . In the row corresponding to an edge e with endpoints i and j (where $i < j$), we have $\mathbf{p}(e)$ in the columns corresponding to i , $-\mathbf{p}(e)$ in the columns corresponding to j , and zeroes in all other entries. Order the rows of the rigidity matrix in the order of the edges of G .

Definition 2.3. We say that an $[a, b]$ -frame $G(\mathbf{p})$ is generically minimally rigid if the associated generic $[a, b]$ -frame $G(\mathbf{x})$ has a rigidity matrix $M(G(\mathbf{x}))$ with rank $kn - k$.

The generic rigidity matrix for the example in Figure 5 is shown below.

$$\begin{array}{l} \text{line-line distance (blind part)} \\ \text{line-line distance (angular part)} \\ \text{point-line distance (non-generic)} \end{array} \begin{pmatrix} A_1 & A_2 & A_3 & B_1 & B_2 & B_3 \\ x_1 & x_2 & x_3 & -x_1 & -x_2 & -x_3 \\ y_1 & 0 & 0 & -y_1 & 0 & 0 \\ z_1 & z_2 & z_3 & -z_1 & -z_2 & -z_3 \end{pmatrix}$$

It has 3 columns for each body, corresponding to the one rotational and two translational degrees of freedom for infinitesimal rigid body motion in the plane. We order the columns so that they are in groups of 3, with translational components last: column A_1 corresponds to the rotational component, and columns A_2 and A_3 to the translational components, with body B 's columns ordered analogously. There is a row for each primitive constraint; notice that that row for the primitive angular constraint associated to the **line-line distance** constraint has zeroes (highlighted in red) in the columns corresponding to the translational degrees of freedom.

2.3. Minimally rigid graphs

A result from [2] gives a combinatorial characterization of generic minimal rigidity for 2D body-and-cad frameworks (with $[1, 2]$ -frames) and, omitting point-point coincidence constraints, for 3D body-and-cad frameworks (with $[3, 3]$ -frames):

⁸The $[a, b]$ -frame defined here is equivalent to the $(a + b, a)$ -frame defined in [2].

Theorem 1. An $[a, b]$ -frame with bi-colored graph $G = (V, E = R \sqcup B)$ is generically minimally rigid if and only if $\exists B' \subseteq B$ such that:

- $(V, R \cup B')$ is the edge-disjoint union of a trees, and
- $(V, B \setminus B')$ is the edge-disjoint union of b trees

Theorem 1 can also be stated in terms of *hereditary sparsity*, which we now recall. A multigraph $G = (V, E)$ is (k, ℓ) -sparse if every subset of n' vertices spans at most $kn' - \ell$ edges; if in addition, G has exactly $kn - \ell$ edges, it is called (k, ℓ) -tight. For brevity, (k, ℓ) -tight graphs will be called (k, ℓ) -graphs. A subset of vertices of G that induces a (k, ℓ) -graph is a (k, ℓ) -block. When $\ell \in [0, 2k]$, (k, ℓ) -graphs are the bases of the (k, ℓ) -matroid [11].

Definition 2.4. Let $G = (V, E = B \sqcup R)$ be a bi-colored graph, a, b be positive integers, and $k = a + b$. Then G is $[a, b]$ -sparse⁹ if $\exists B' \subseteq B$ such that:

- $(V, R \cup B')$ is (a, a) -sparse, and
- $(V, B \setminus B')$ is (b, b) -sparse

Additionally, if G has exactly $kn - k$ total edges, then G is $[a, b]$ -tight and referred to as an $[a, b]$ -graph.

A subset of vertices of an $[a, b]$ -sparse graph that induces an $[a, b]$ -graph is an $[a, b]$ -block.

The Nash-Williams and Tutte Theorem [18, 19] states that G is a (k, k) -graph if and only if G is the edge-disjoint union of k spanning trees. Therefore, the $[a, b]$ -graph property is equivalent to there existing $B' \subseteq B$ such that $(V, R \cup B')$ is the edge-disjoint union of a spanning trees and $(V, B \setminus B')$ is the edge-disjoint union of b spanning trees.

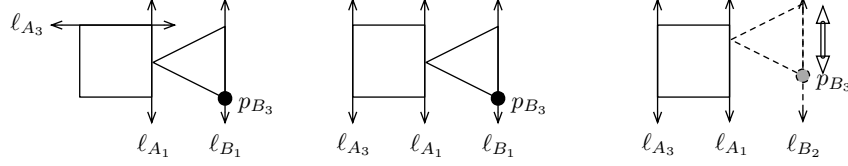
That this class is matroidal follows from the Matroid Union Theorem [20, Prop. 7.6.14]. Therefore, for an $[a, b]$ -sparse graph $G = (V, E)$ and an edge e not in E , we will say that e is *independent* of G if $G + e$ is also $[a, b]$ -sparse and *dependent* otherwise.

2.4. Non-genericity

While the rank of a generically minimally rigid framework is $kn - k$ for almost all realizations, there are realizations for which the rank drops. These correspond to non-generic realizations, or *special positions*, of the generically minimally rigid graph.

In Figure 7 we consider a special position of the framework specified by the graph from Figure 5. By changing the choice of placement for the line on body

⁹As we will rely on both concepts of sparsity, we draw the reader's attention to the use of **parentheses** to denote the parametrized (k, ℓ) -sparsity of simple graphs (appearing for classical bar-and-joint and body-and-bar rigidity) and the use of **square brackets** to denote the parametrized $[a, b]$ -sparsity counts of bi-colored graphs (introduced for body-and-cad rigidity).



(a) As in Figure 5, we specify a **point-line distance** constraint that requires point p_{B_3} on the triangle to be a fixed distance from line ℓ_{A_3} on the square. The resulting (generic) framework is minimally rigid.

(b) An alternative choice of the line on body A involved in Constraint II.

(c) The resulting flexible non-generic framework admits an internal motion with 1 degree of freedom.

Figure 7: A **flexible special position** of a generically minimally rigid 2D body-and-cad framework.

A in the final constraint, we have constructed a non-generic realization of the framework which has a consistent dependency and remains flexible.

Its rigidity matrix is shown below and contains a dependency (the third row is the sum of the first two), causing its pure condition to vanish.

	A_1	A_2	A_3	B_1	B_2	B_3
point-line coincidence	1	0	-1	-1	0	1
line-line perpendicular	-1	0	0	1	0	0
point-line distance (non-generic)	0	0	-1	0	0	1

3. Structure of the pure condition

In this section, we review the definition of a polynomial called the pure condition that is associated to a body-and-cad framework. If G is a minimally rigid graph and \mathbf{p} is generic, the kernel of $M(G(\mathbf{p}))$ contains exactly the space of trivial infinitesimal motions of $G(\mathbf{p})$, corresponding to rigid-body motions of the entire framework as a single unit. To remove these, we choose some i with $1 \leq i \leq n$, and construct the *standard tie-down* at body i by appending to $M(G(\mathbf{p}))$ a $k \times kn$ matrix whose only nonzero entries are given by the identity matrix in the k columns associated to body i .¹⁰ We denote the rigidity matrix of $G(\mathbf{p})$ with a tie-down by $M_T(G(\mathbf{p}))$.

Definition 3.1. *The pure condition P_G of a tied down $[a, b]$ -graph G is the determinant of $M_T(G(\mathbf{x}))$.*

¹⁰The notion of tie-downs can be substantially generalized to generic tie-downs of any $[a, b]$ -sparse graph. For our purposes, this would only complicate the notation, so we restrict our attention to standard tie-downs.

The pure condition depends, a priori, on the choice of tie-down of G . We will show that as in the body-bar setting of [8], this dependence can be removed.

Theorem 2. *The pure condition of a tied down $[a, b]$ -graph G is non-zero for any choice¹¹ of the tie down and has the form $P_G = T_G \cdot C_G$, where T_G depends on the tie down and C_G is independent of the tie down.*

This result follows from two combinatorial formulas for the pure condition that we derive below. Since the proofs are relatively standard and similar to what can be found in [8, 21], we develop them quickly.

Tree decompositions.

Let G be an $[a, b]$ -graph. A *tree decomposition* $\mathcal{T} = (A_1, \dots, A_a, T_1, \dots, T_b)$ of G is a partition of the edges into k spanning trees such that all the red edges are in the sets A_i . It follows from the definitions in Section 2.3 that there is a tree decomposition of a bi-colored graph if and only if it is an $[a, b]$ -graph.

To make the connection to the pure condition we define the *tree decomposition monomial* $\{\mathcal{T}\}$ to be

$$\{\mathcal{T}\} := \prod_{e \in A_i, i \in [a]} \mathbf{x}(e)_i \prod_{e \in T_j, j \in [b]} \mathbf{x}(e)_{a+j}$$

The tree monomials are precisely the monomials appearing in P_G . We first give a concrete example before stating the general theorem.

Example 3.2. Let G be the $[2, 2]$ -graph on vertices 1 and 2 with two red edges and two black edges depicted in Figure 3.2.

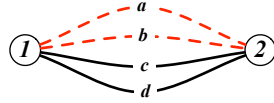


Figure 8: A $[2, 2]$ -tight graph on vertices 1 and 2 with two red (dashed) edges a and b and two black (solid) edges c and d .

The tied down rigidity matrix is

$$\begin{pmatrix} a_1 & a_2 & 0 & 0 & -a_1 & -a_2 & 0 & 0 \\ b_1 & b_2 & 0 & 0 & -b_1 & -b_2 & 0 & 0 \\ c_1 & c_2 & c_3 & c_4 & -c_1 & -c_2 & -c_3 & -c_4 \\ d_1 & d_2 & d_3 & d_4 & -d_1 & -d_2 & -d_3 & -d_4 \\ 1 & 0 & 0 & 0 & 0 & 0 & 0 & 0 \\ 0 & 1 & 0 & 0 & 0 & 0 & 0 & 0 \\ 0 & 0 & 1 & 0 & 0 & 0 & 0 & 0 \\ 0 & 0 & 0 & 1 & 0 & 0 & 0 & 0 \end{pmatrix}$$

¹¹The standard tie-down pins k coordinates of one body, but we can also choose “generic” tie-downs that pin k coordinates chosen from different bodies.

There are 4 tree decompositions:

$$(\{a\}, \{b\}, \{c\}, \{d\}), (\{b\}, \{a\}, \{c\}, \{d\}), (\{a\}, \{b\}, \{d\}, \{c\}), (\{b\}, \{a\}, \{d\}, \{c\}).$$

The corresponding monomials give the determinant of the rigidity matrix with a standard tie-down: $a_1b_2c_3d_4 - a_2b_1c_3d_4 - a_1b_2c_4d_3 + a_2b_1c_4d_3$.

□

Theorem 3. *If G is a tied down $[a, b]$ -graph*

$$P_G = \sum_{\substack{\text{tree decomp.} \\ \mathcal{T}}} \pm\{\mathcal{T}\} \quad \text{in } \mathbb{R}[\mathbf{x}]. \quad (1)$$

The signs can be determined using the definition of the determinant of a matrix. The precise formula for the signs is technical and not needed in what follows, so we do not describe it here.

Proof. We sketch a proof that follows the proof of Theorem 2.18 in [8]. First we reorder the columns of $M_T(G(\mathbf{x}))$ by the coordinates of $\mathbf{p}(e)$ so that we have the n first coordinates, followed by the n second coordinates, etc. In doing this we can see that if we ignore the last k rows corresponding to the tie down, each successive collection of n columns is just an incidence matrix for the directed multigraph G whose rows are the edges of G , and whose columns correspond to the vertices.

We expand the determinant of $M_T(G(\mathbf{x}))$ along these successive groups of n columns. To do this, in each set of n columns, we need to choose n rows. Since this set of n columns is an incidence matrix, if this subdeterminant is nonzero, then these rows must correspond to a spanning tree plus a row corresponding to the tie down. Moreover, this subdeterminant is actually a monomial as it is possible to expand it row by row, choosing the tie down as the first row, choosing an edge incident to the tied-down vertex as the next row, and choosing successive rows by taking an edge that was adjacent to an edge already chosen. Proceeding in this way, each row that we choose has only one nonzero entry.

The resulting $n \times n$ determinant is multiplied by k others, all chosen in the same way, to obtain a monomial. Since we cannot permit any row to appear twice in such a product, this product of k $n \times n$ determinants corresponds to a decomposition of G into k edge-disjoint spanning trees.

Moreover, we argue that such a product is nonzero if and only if the k trees form an $[a, b]$ -tree decomposition. To see this, note that within the last b groups of n columns, the rows corresponding to red edges have only zeroes as entries. So, all of the red edges are in the a trees corresponding to the first a coordinates.

□

In particular, since the tree decompositions are independent of the tie-down, P_G is determined up to sign. We define the *critical factor*¹² C_G to be P_G with

¹²The name comes from the setting of general tie-downs, where ± 1 is replaced with the determinant of a $k \times k$ matrix.

respect to the tie-down that pins vertex 1, to establish a convention.

Fans.

An alternative combinatorial formula generalizes one based on the k -fans of [8]. Fix the ordering and base orientation of the edges as in Definition 2.2, where edges are oriented from i to j if $i < j$. The ordering on the edges induces an ordering on subsets. For a tied-down $[a, b]$ -graph, an $[a, b]$ -fan \mathcal{F} is an orientation of the edges such that: (a) all edges incident to the tied-down vertex i are oriented toward i ; (b) at all other vertices, exactly k edges are oriented out, at most a of which are red. Define F_j to be the set of edges oriented out of vertex j . The sign $\varepsilon(\mathcal{F})$ is $(-1)^t$, where t is the number of edges oriented opposite to the base orientation by \mathcal{F} . We define the *fan monomial* $[\mathcal{F}]$ by

$$[\mathcal{F}] := \text{sgn}(\sigma)\varepsilon(\mathcal{F}) \prod_{j \in [n] \setminus \{i\}} [F_j]$$

where $[F_j]$ is the *bracket* associated to the (ordered) set of vectors $\mathbf{x}(e)$ for $e \in F_j$ and σ is the permutation of the edges that puts them in the order F_1, F_2, \dots, F_n . The brackets can be thought of either as elements of the homogeneous coordinate ring of the Grassmannian, or simply as the determinant of the $k \times k$ matrix with columns $\mathbf{x}(e)$.

It is not hard to check the following, which is a generalization of Proposition 2.12 in [8].

Theorem 4. *For a tied-down $[a, b]$ -graph, G , we have*

$$P_G = \sum_{\substack{[a, b]\text{-fans} \\ \mathcal{F}}} [\mathcal{F}]. \quad (2)$$

Example 3.3 (Example 3.2, continued). If G is the graph on two vertices in Figure 3.2, and we tie down vertex 1, we see that there is a unique $[2, 2]$ -fan with all four edges pointing from vertex 2 to vertex 1. Hence, $P_G = [abcd]$, and even in this very simple example, we can see how expressing P_G in terms of brackets greatly simplifies notation. \square

4. Factors of the pure condition and factor graphs

In this section, we investigate the structure of factors of the (critical factor of the) pure condition of an $[a, b]$ -graph. The goal is to identify these factors graph-theoretically. This is more complicated than in the body-and-bar setting where irreducible factors correspond to rigid subgraphs. In our case we will have some factors that correspond to rigid $[a, b]$ -subgraphs, some that correspond to rigid (a, a) or (b, b) -subgraphs, and others that cannot be interpreted as the pure condition of any rigid subgraph.

For the rest of this section G will refer to an $[a, b]$ -graph, so that C_G is well-defined. To further understand the structure of the pure condition, we may

contract subgraphs. If H is a subgraph of G , we write G/H to denote the graph obtained by deleting the edges of H and identifying the vertices of H .

Definition 4.1. Let G be an $[a, b]$ -graph with pure condition $C_G = fg$. We say that the edge support of the factor f is the set E_f of edges e in G such that some variable of $\mathbf{x}(e)$ is in f .

The supports of distinct factors define edge-disjoint subgraphs of G .

Theorem 5. Let $C_G = fg$. Then the edge supports of f and g are disjoint and partition $E(G)$. Moreover, every monomial of a factor contains exactly one coordinate from each edge in its support.

Proof. From Equation (1) we can see that every monomial of C_G contains exactly one coordinate from each edge. If the coordinates of $\mathbf{x}(e)$ were split between two distinct factors, then their product would have terms divisible by more than one coordinate of $\mathbf{x}(e)$, which would be a contradiction. \square

Theorem 5 allows us to make the following definition.

Definition 4.2. A bi-colored graph H is a factor graph of G if H is a minor¹³ of G and $C_G = hf$, with the factor h supported on H . The factor graph H is proper, if $h = C_H$ for some tie down of H . If H is all red we abuse notation and consider it as an (a, a) -graph. If H is a black (b, b) -graph whose vertices are contained in a red (a, a) -graph, then we consider H as a (b, b) -graph labeled by the last b coordinates of the edge vectors.

Example 4.3 (Example 3.2, continued again). Define H to be the subgraph of G containing the two red edges. Then H is a proper factor graph as it is the pure condition of this graph as a $(2, 2)$ -graph. The black factor graph consisting of the other two edges is also proper, though its edges are now labeled by the 2-vectors (c_3, c_4) and (d_3, d_4) .

Here we note two key differences between $[a, b]$ -graphs and (k, k) -graphs and discuss their consequences. First, in the pure condition of a (k, k) -graph, if e is an edge, every coordinate of $\mathbf{x}(e)$ appears in some monomial in the pure condition. In this example, c_1, c_2, d_1 , and d_2 do not divide any monomial. Second, in the (k, k) -graph setting, each irreducible factor is the pure condition of a (k, k) -graph. In our example, P_G factors as $(a_1b_2 - a_2b_1)(c_3d_4 - c_4d_3)$, yet neither factor is the pure condition of an $[a, b]$ -subgraph of G . \square

This next theorem gives a first indication of why it is convenient to define factor graphs in terms of minors instead of, e.g., subgraphs or subset of edges, as we see that C_G may factor as the product of the pure condition of a proper subgraph H and the pure condition of G/H , the minor obtained by contracting H . The geometric meaning of Theorem 6 is that, if H corresponds to a rigid

¹³Graph minors are obtained by deleting edges and vertices and contracting edges.

sub-framework (i.e., an $[a, b]$ -subgraph), we can split the special positions of G into two types: (i) special positions of H , which induce special positions of G ; (ii) special positions of G where H is placed generically. In case (ii), H can be replaced by a single rigid body, so these special positions are special positions of G/H . Theorem 6 is a small modification of [8, Theorem 4.12] to body-and-cad.

Theorem 6. *Let G have a proper subgraph H that is an $[a, b]$ -block. Then H and G/H are both proper factor graphs and $C_G = C_H \cdot C_{G/H}$.*

The proof requires the following standard lemma.

Lemma 4.4. *Let G be a (k, k) -graph, and let H be a proper block. Then G/H is also a (k, k) -graph.*

Proof. Fix a tree decomposition T_1, \dots, T_k of G , and let n' be the number of vertices of H . Since H has $m' = kn' - k$ edges, all of which are covered by one of the trees, $|T_i \cap H| = n' - 1$ for every i . Thus, contracting H involves contracting a subtree of each of the T_i . Since contracting a connected subtree of any tree T produces a smaller tree T' , contracting H produces a set of k trees that cover the edges of G/H . By the Tutte-Nash-Williams Theorem G/H is also a (k, k) -graph. \square

Proof of Theorem 6. Since H is an $[a, b]$ -graph, it has a pure condition C_H . Lemma 4.4 then implies that G/H is also an $[a, b]$ -graph, so $C_{G/H}$ is defined as well. If both C_H and $C_{G/H}$ divide C_G , then $C_G = C_H \cdot C_{G/H}$, since the supports of H and G/H are disjoint and partition the edges of G .

To see that C_H and $C_{G/H}$ divide C_G , we will use Equation (1), and a small elaboration of the proof of Lemma 4.4. Pick tree decompositions \mathcal{T}_H and $\mathcal{T}_{G/H}$ of H and G/H . Suppose that the union T of T_1^H and $T_1^{G/H}$ contains a cycle in G . Since T_1^H is a tree, this cycle is not contained entirely in H . This implies that $T/T_1^H = T_1^{G/H}$ is not acyclic, which is a contradiction.

Because \mathcal{T}_H and $\mathcal{T}_{G/H}$ were arbitrary, a tree decomposition of G is determined by picking one of H and G/H independently. The desired result then follows from Equation (1). \square

It is not too hard to see that for a body-and-bar framework every factor graph is proper. The next few theorems indicate that body-and-cad is more complicated than body-and-bar.

Theorem 7. *Let G be an $[a, b]$ -graph with a subgraph H that contains only red edges and is an (a, a) -block. Then H is a proper factor graph of G .*

Proof. Because H is a completely red (a, a) -block, any tree decomposition decomposition of G induces a decomposition of H into a edge-disjoint spanning trees. The trees covering H can be chosen independently of the trees covering the remaining edges, so the theorem follows from Equation (1). \square

Figures 11 and 14 contain two examples with red (a, a) -blocks appearing as proper factor graphs. The geometric interpretation of Theorem 7 is that as a sub-framework H is not rigid, but *angularly rigid*: only translational degrees of freedom are permitted between the vertices spanned by H . In light of this, we define the following.

Definition 4.5. *Let G be $[a, b]$ -sparse. If H is a subgraph that contains only red edges and is an (a, a) -block, we say that it is an angular block. If G is an $[a, b]$ -graph, then an angular block is an angular factor graph.*

A key difference between the situation in Theorem 6 and that of Theorem 7 is that we cannot simply contract H and obtain another proper factor graph. Indeed, as the example in Figure 12 shows, $G \setminus H$ may be an *improper* factor graph, indicating that the distinction is necessary.

So far we have seen four types of proper factor graphs – $[a, b]$ -subgraphs, quotients of $[a, b]$ -subgraphs, all red (a, a) -subgraphs and all black (b, b) -subgraphs (as in Example 4.3). Before giving the detailed context in which black (b, b) -subgraphs may be proper factor graphs, which is quite technical, we provide the geometric intuition. Refer back to the example in Figure 1(b). Suppose that G contains an angular factor H (parallel constraints in the example). As previously described, the vertices spanned by H (A , B and C in the example) are “translating bodies” relative to each other; then, a (b, b) -block J on a subset of the vertices of H (B and C in the example) will, in fact, completely rigidify them. This will hold *even if the vertex set of J does not induce an $[a, b]$ -block*, which implies that body-and-cad, even in the plane, allows us to construct frameworks with generically rigid components that are not rigid as induced subgraphs.

Definition 4.6. *Let G be an $[a, b]$ -sparse graph with an angular factor graph H , and let J be a (b, b) -block on a subset of the vertices of H . If J does not span all the vertices of H , then J is a contextually rigid component.*

By analogy with the geometric reasoning used to identify the factor graph associated with an $[a, b]$ -block, we want to think of the vertices of J as corresponding to a single rigid body. While we previously continued by looking for proper factor graphs in G/J , a more complicated construction is required when J does not span an $[a, b]$ -block.

Theorem 8. *Let G be an $[a, b]$ -graph with an all red (a, a) -block H as a subgraph and an all black (b, b) -block J with $V(J) \subset V(H)$. Tie down a vertex in J , fix an $[a, b]$ -tree decomposition \mathcal{T} of G , and orient all edges towards this root. Define G' by removing all of the edges of H whose tails are in J and then contracting J . Then,*

1. H and J are proper factor graphs
2. $C_G = C_H \cdot C_J \cdot f$, where f is supported on a subgraph F whose edges are the edges of G that are not in H or J .
3. G' is an $[a, b]$ -graph with $C_{G'} = hf$, where h is supported on the red (a, a) -block $H' = H/J$.

Proof. That H is a factor graph of G follows from Theorem 7. To see that J also is, observe that, since $V(J) \subset V(H)$, all the edges of J are covered by trees T_j (and not A_i). Thus, the decomposition of J into b trees is independent of the rest of any tree decomposition. Hence, C_J (the pure condition of a (b, b) -graph) divides C_G , using the same arguments as above.

To show that G' is an $[a, b]$ -graph, we will show that \mathcal{T} restricts to an $[a, b]$ -tree decomposition of G' . In each tree there was a unique directed path from each vertex in G to the root in J . Since our construction only deletes edges directed out of J , there is still a unique directed path in each tree from each vertex remaining in G' to the root. If an undirected cycle were created in this process, it is easy to see that there would have also been an undirected cycle in the original tree. Therefore, the restriction of \mathcal{T} to \mathcal{T}' in G' is an $[a, b]$ -tree decomposition.

Finally, we argue that $H' = H/J$ is a red (a, a) -block in G' . This will imply that H' is a factor graph of G' , yielding the last assertion of the theorem. Above, we argued that the a red trees of \mathcal{T} in H restrict to a red trees in \mathcal{T}' in H' . By Nash-Williams-Tutte, H' is a (a, a) -block (of all red edges). By Theorem 7, H' is a proper factor graph of G' and $C_{G'} = hf$ with h supported on H' . \square

5. Algorithms for detecting dependencies

We now present combinatorial algorithms to aid in detecting dependencies in CAD systems. The first algorithm, the $[a, b]$ -**pebble game**, characterizes $[a, b]$ -sparsity and consequently addresses *generic* body-and-cad rigidity. If the addition of an edge results in a dependency in a generic realization of the system, the pebble game will find its fundamental circuit. The second set of **factor graph algorithms** determines the proper and improper *factor graphs* for an $[a, b]$ -graph, which correspond to factors of its pure condition. When the geometry of a CAD system causes any of these factors to vanish, the system is in a *special position* and contains a dependency.

5.1. Pebble games for $[a, b]$ -sparsity

Generic minimal rigidity of body-and-cad frameworks is characterized by $[1, 2]$ -sparsity in the plane and, omitting point-point coincidence constraints, $[3, 3]$ -sparsity in 3D [2].

Algorithm 1 describes our $[a, b]$ -*pebble game* for solving the **Decision**, **Extraction**, **Components** and **Optimization** algorithmic problems described in [11] for $[a, b]$ -sparse graphs as well as detecting the fundamental circuit of a dependent edge. This algorithm belongs to a family of pebble game algorithms [22, 11] that are based on a set of local moves applied to the edges of a directed graph, where the edges and vertices are covered by pebbles representing degrees of freedom. The specific preconditions for each type of move, which are related to the sparsity parameters, determine the sparsity family recognized by the game.

One way of intuitively understanding the $[a, b]$ -pebble game is to imagine separate (a, a) - and (b, b) - pebble games played on sets A and T , which partition

Algorithm 1 The $[a, b]$ -pebble game algorithm.

Input: A bi-colored graph $G = (V, E = B \sqcup R)$, with black B and red R edges.

Output: $[a, b]$ -sparsity property **tight**, **sparse**, **dependent** and **contains spanning tight**, or **dependent**.

Setup: Initialize an empty directed graph H on vertex set V . On each vertex, place a aqua pebbles and b tan pebbles.

Allowed moves:

Add red edge ij [Precondition: $\geq a + 1$ aqua pebbles on i and j .]

– Add the new edge, cover it with an aqua pebble from i (there is one by the precondition).

– Orient ij out of i .

Add black edge ij [Precondition: $\geq a + 1$ aqua pebbles on i and j or $\geq b + 1$ tan pebbles on i and j .]

– Add the new edge; cover it with a pebble from i using aqua (if there are $a + 1$ aqua) or tan (if there are $b + 1$ tan).

– Orient ij out of i .

Edge reversal [Precondition: vertex j has a pebble on it and an in-edge ij covered by the same color.]

– Reverse the edge by orienting it as ji out of j , covering with the pebble from j and returning the (same color) pebble originally covering ij to i .

Aqua exchange edge reversal [Precondition: vertex j has an aqua pebble on it and a black in-edge ij covered by a tan pebble; i and j do not belong to the same (a, a) -component of aqua pebble covered edges.]

– Reverse the edge by orienting it as ji out of j , covering with the aqua pebble from j and returning the tan pebble originally covering ij to i .

Tan exchange edge reversal [Precondition: vertex j has a tan pebble on it and a black in-edge ij covered by an aqua pebble; i and j do not belong to the same (b, b) -component of tan pebble covered edges.]

– Reverse the edge by orienting it as ji out of j , covering with the tan pebble from j and returning the aqua pebble originally covering ij to i .

Method:

1. For each edge $e \in E$
 - (a) If e is black: attempt to collect $b + 1$ tan pebbles on its endpoints with Alg. 2.
 - (b) If Alg. 2 returns **true**: insert e with an **add black edge** move.
 - (c) Else, or if e is red: attempt to collect $a + 1$ aqua pebbles on its endpoints with Alg. 2.
 - (d) If Alg. 2 returns **true**: insert e with an **add black/red edge** move.
 - (e) Else: *reject* it and highlight the edges returned by Alg. 2 as the fundamental circuit of the edge (if e is black, this is the union of both calls to Alg. 2).
 2. If every edge is added: output **tight** if there are $a + b$ pebbles left and **sparse** otherwise.
 3. Else, there were rejected edges: output **dependent and contains spanning tight** if there are $a + b$ pebbles left and **dependent** otherwise.
-

Algorithm 2 The subroutine for finding pebbles for the $[a, b]$ -pebble game.

Input: An $[a, b]$ -pebble game configuration (a directed bi-colored graph), an edge e , and a desired additional pebble color c_e (**aqua** or **tan**).

Output: **true** if $a + 1$ aqua (if c_e is aqua) or $b + 1$ tan (if c_e is tan) pebbles can be collected on the endpoints of e or **false** otherwise, along with the set of visited edges.

Method:

1. Initialize set $F = \emptyset$.
 2. Initialize queue $Q = \emptyset$. Entries of Q will be of the form (f, c) , recording an edge on which to cover with a pebble of color c .
 3. Set $e.predecessor = \text{NIL}$.
 4. Enqueue (e, c_e) into Q .
 5. While Q is not empty
 - (a) Dequeue (f, c) .
 - (b) If $f \neq e$ and f is red, continue to the next iteration of the loop.
 - (c) Use the basic pebble game rules to try to collect $a + 1$ (if c is **aqua**) or $b + 1$ (if c is **tan**) pebbles on the endpoints of f ; let F' be the set of edges visited by that search.
 - (d) If the pebbles were collected
 - i. Let $g = f$.
 - ii. While $g.predecessor \neq \text{NIL}$
 - A. Let d be the color of the pebble covering g , \bar{d} be the opposite color, u and v the source and target of g .
 - B. Collect a pebble of color \bar{d} on v using the basic pebble game rules with **edge reversal** moves.
 - C. Perform a \bar{d} **exchange edge reversal** move to reverse the edge from v to u , covering it with the \bar{d} -colored pebble and releasing a d -colored pebble back onto u .
 - D. Set $g = g.predecessor$.
 - iii. Collect $a + 1$ (if c is **aqua**) or $b + 1$ (if c is **tan**) pebbles on the endpoints of $g(= e)$.
 - iv. Output **true** and $F \cup F'$.
 - (e) Otherwise
 - i. For each edge $g \in F'$ that is not in F
 - A. Set $g.predecessor = f$; let \bar{c} be the opposite of color c .
 - B. Enqueue (g, \bar{c}) into Q .
 - ii. Assign $F = F \cup F'$.
 6. Output **false** and F .
-

the current edge set, respectively. The aqua-colored pebbles track the edges in A as well as the (a, a) -sparsity of that partition; the tan-colored pebbles do the same for T with (b, b) -sparsity counts¹⁴. The $[a, b]$ -pebble game relies on moves that permit black edges to move between A and T in a controlled manner, which corresponds to collecting additional pebbles of certain colors, using a subroutine described in Algorithm 2. To find a sequence of these moves, Algorithm 2 specializes Knuth’s matroid union algorithm [16] to the $[a, b]$ -sparsity matroid using pebble games. By enqueueing unvisited edges (in $F' \setminus F$), it uses a breadth-first approach to find the shortest path (stored with *predecessor* pointers) to an edge whose pebble color can be exchanged. To help illustrate the algorithm, Figure 9 shows some steps of the pebble game played on the primitive cad graph for Figure 2.

5.2. Correctness

We now show correctness of Algorithm 1.

Theorem 9. *A bi-colored graph is $[a, b]$ -sparse if and only if it can be constructed with the $[a, b]$ -pebble game.*

We are going to prove that Algorithm 1 correctly characterizes $[a, b]$ -sparse graphs and that it can be used to find circuits. Structurally, the search procedure in Algorithm 2 corresponds to Knuth’s [16] algorithm for matroid union (see [23, Sec. 42.3] for a modern treatment). Thus, one can infer correctness once this equivalence is established. However, for clarity, we will first prove that any graph constructed with the moves described in Algorithm 1 is $[a, b]$ -sparse.

In what follows, we describe a pebble game configuration as (H, A, T) , where H is a bi-colored directed graph on vertex set V , with a pebble covering every edge and some free pebbles on vertices; A is the set of edges covered by aqua pebbles and T is the set of edges covered by tan pebbles. We will also abuse notation slightly and use the same symbols H , A , and T to describe their underlying undirected graphs. Finally, we will use the notation $S + e$ to denote $S \cup \{e\}$ and $S - e$ to denote $S \setminus \{e\}$.

Lemma 5.1. *The underlying graph of any pebble game configuration is $[a, b]$ -sparse with A as an (a, a) -sparse graph and T as a (b, b) -sparse graph.*

Proof. We show something slightly stronger, which is that the underlying graph H constructed by applying *any sequence* (as opposed to only the ones found by the algorithm) of the pebble game moves is always $[a, b]$ -sparse.

The key invariant is that, after any sequence of moves, A and T both induce pebble game configurations for the *basic* (uncolored) pebble game from [11]. As an immediate consequence, we obtain that A remains (a, a) -sparse and B

¹⁴We chose the colors aqua and tan to be associated with A and T ; in the rigidity setting, the aqua-covered A partition can be thought of as tracking the angular degrees of freedom of the system, while the tan-colored T partition tracks the translational degrees of freedom.

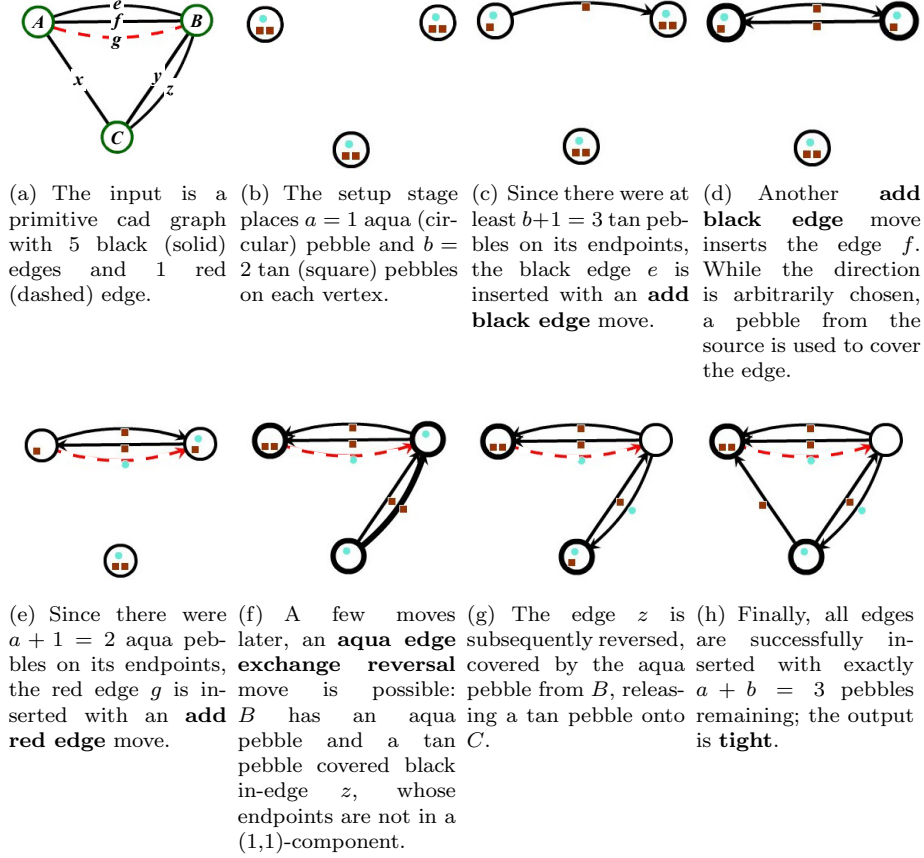


Figure 9: The $[a, b]$ -pebble game (Algorithm 1) played on a primitive cad graph for a generically minimally rigid framework determines that it is $[1, 2]$ -tight.

remains (b, b) -sparse. This certifies that H is $[a, b]$ -sparse. The invariant clearly holds at initialization, so we proceed by induction on the number of moves.

For the inductive step, we first consider all the moves except for the **exchange edge reversal** moves. We observe that, assuming the required preconditions, these operate entirely on either A or T as a configuration, so the inductive step for them follows directly from [11].

To complete the induction, consider the **aqua edge exchange reversal** move, since the tan one has an analogous proof. The precondition, that the edge $ij \in T$ is not in an (a, a) -component of A , implies that $A + ij$ is (a, a) -sparse. From this, the pebble game invariants of [11] imply that there are a aqua pebbles (distinct from the one on j) reachable from i via paths using only edges in A . By induction, A could have been built by the basic (a, a) -pebble game; then ij could be added to A by basic pebble game searches. Notice that returning the tan-colored pebble to j maintains T as a basic (b, b) -pebble game

configuration. □

The other direction is captured by the following lemma.

Lemma 5.2. *If an edge is independent of the underlying graph of a pebble game configuration, then the pebble game will successfully insert it.*

Before giving the proof, we briefly review Knuth’s algorithm and establish some terminology, specialized to our setup. The algorithm operates on a directed, bipartite graph associated with a pebble game configuration (H, A, T) and an edge e , which is not in H . This graph, denoted Γ_{H+e} , has vertex set given by the edges of H , i.e., $A \sqcup T$, along with two *terminal* vertices α and τ , and an additional vertex for the edge e . First, we describe the edges originating and terminating at a vertex $x \notin \{e, \alpha, \tau\}$.

There is a directed edge from vertex x to y , written $x \rightarrow y$ if

$$\left\{ \begin{array}{ll} (A - y) + x \text{ is } (a, a)\text{-sparse} & \text{if } x \in T \text{ \& } y \in A \\ (T - y) + x \text{ is } (b, b)\text{-sparse} & \text{if } y \in T \text{ \& } x \in A \cap B, \text{ i.e.,} \\ & x \text{ is a black edge in the aqua partition} \end{array} \right.$$

Additionally, there is an edge $x \rightarrow \alpha$ if $x \in T$ and $A + x$ is (a, a) -sparse, and there is an edge from $x \rightarrow \tau$ if $x \in A \cap B$ and $T + x$ is (b, b) -sparse. The edges originating at e are defined similarly. This case distinction is simply to make it clear that no edges in Γ_{H+e} have e as their target.

A path $x_0 \rightarrow x_1 \rightarrow \dots \rightarrow x_\pi$ has a *shortcut* in a graph if there exists a $j > i + 1$ such that $x_i \rightarrow x_j$ is an edge. In particular, if $x_0 \rightarrow x_1 \rightarrow \dots \rightarrow x_\pi$ is a shortest path in a graph, it does not have a shortcut.

Given a path from e to a terminal vertex, *recoloring along the path* means putting x_i in the part of the partition containing x_{i+1} , with α always in A and τ always in T .

The main result of [16], again specialized for our setup, is:

Theorem 10. *Let (H, A, T) be a pebble game configuration and e an edge not in the underlying graph. Then there is a directed path in Γ_{H+e} from e to α or τ if and only if $H + e$ is independent. Moreover, given a path $e = x_0 \rightarrow x_1 \rightarrow \dots \rightarrow x_\pi \in \{\alpha, \tau\}$ in Γ_{H+e} that does not have a shortcut, a partition of $H + e$ certifying $[a, b]$ -sparsity can be found by recoloring along this path.*

The proof of Lemma 5.2 amounts to showing that Algorithm 2 is simulating Knuth’s algorithm.

Proof of Lemma 5.2. Assume that e is independent of the underlying graph of a pebble game configuration H . We need to show that Algorithm 2 will succeed in collecting enough pebbles on the endpoints of e . This is done by comparing the pebble search procedure in Algorithm 2 to Knuth’s algorithm.

First consider, in the main loop of Algorithm 2, the conditional block predicated upon when $a + 1$ (if c is aqua) or $b + 1$ (if c is tan) pebbles can be collected on the endpoints of f . Note that a aqua or b tan pebbles can always be collected

on any vertex by [11]. The additional pebble can be collected if and only if the edge f can be moved to the opposite part of the partition without violating sparsity. This is equivalent to there being an edge $f \rightarrow \{\alpha, \tau\}$ in Γ_{H+e} .

Otherwise, the pebble search fails. In this case, [11] implies that $F' + f$ is the fundamental circuit of f in the c -colored part of the partition; i.e., $g \in F'$ if and only if there is an edge $f \rightarrow g$ in Γ_{H+e} . Therefore, F' is exactly the set of neighbors of f in Γ_{H+e} .

By enqueueing those edges in F' not already in F , Algorithm 2 is, in fact, searching Γ_{H+e} in a breadth-first fashion. By Theorem 10, the assumption that $H + e$ is $[a, b]$ -sparse implies that there is a path from e to a terminal vertex in Γ_{H+e} . Therefore, Algorithm 2 will be able to collect $a + 1$ aqua or $b + 1$ pebbles on the endpoints of some edge f , implying that there is an edge from f to a terminal in Γ_{H+1} . Let p be the path in Γ_{H+e} defined by following predecessor pointers from f . Since Algorithm 2 implements breadth-first search on Γ_{H+e} , p is shortcut free.

Theorem 10 then implies that recoloring along p preserves the (a, a) - and (b, b) -sparsity of A and T at every step. The main results of [11] then imply that it will always be possible to meet the preconditions of the **exchange edge reversal** moves to implement the recoloring by using only basic pebble searches on A or T . Thus, the pebble game moves implementing the recoloring along p will succeed, and the $[a, b]$ -pebble game will insert e . \square

5.3. Circuits

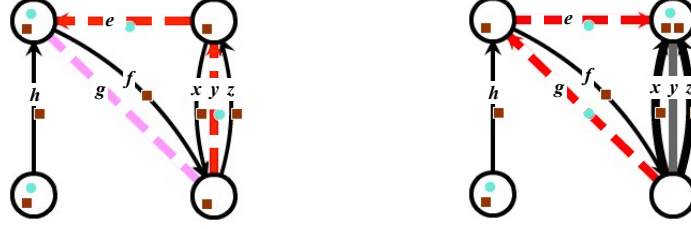
The pebble game also detects $[a, b]$ -circuits, an approach that is perhaps less well-known, but appears before in [11, Section 6] and has been used in [24]. Note that the presence of red edges create the possibility of many types of circuits. Some may be circuits as uncolored $(a+b, a+b)$ graphs, and others may be (a, a) -circuits, but there are other types. The examples in Figure 10 demonstrate a property of circuits that does not arise in the (k, ℓ) -sparsity matroids. While every (k, ℓ) -circuit is (k, ℓ) -spanning, or “rigid,” an $[a, b]$ -circuit may actually be “flexible.” Dropping an edge of a (k, ℓ) -circuit always results in a tight graph, but dropping an edge of an $[a, b]$ -circuit can result in a sparse (but not tight) graph.

Whenever we fail to insert an edge we can use Algorithm 2 to find its fundamental circuit.

Lemma 5.3. *Let F be the set of edges returned by Algorithm 2. The fundamental circuit of e in the configuration graph H is $F + e$.*

Proof. We must show that $F + e$ is dependent and that, for any $y \in F$, $F + e - y$ is independent. Observe that $F + e$ corresponds to the set of vertices reachable from e in the Knuth graph Γ_{H+e} . By the definition of F , every directed path in Γ_{H+e} that starts at e is contained in Γ_{F+e} . Therefore, there is no path from e to a terminal in Γ_{F+e} , and Theorem 10 implies that $F + e$ is not $[a, b]$ -sparse.

Now, let $y \in F$. By construction of F , y is on a short-cut free directed path starting at e . Therefore, there is an $x \in F + e$ on this path with $x \rightarrow y$ and



(a) The fundamental $[1, 2]$ -circuit for rejected edge g detected by the pebble game is the set of edges $\{e, g, y\}$. The set $\{e, y\}$ forms an angularly rigid block.

(b) The fundamental $[1, 2]$ -circuit for rejected edge y detected by the pebble game is the set of edges $\{e, g, x, y, z\}$. The set $\{x, z\}$ forms a contextually rigid block due to the presence of the angular block $\{e, g\}$.

Figure 10: Unlike (k, ℓ) -circuits, removing any edge from a $[1, 2]$ -circuit may not produce a $[1, 2]$ -graph.

edge of Γ_{H+e} . By definition, removing y results in an edge from x to a terminal, providing a path from e to a terminal. In other words, $F + e - y$ is $[a, b]$ -sparse for all $y \in F$, which completes the proof of correctness. \square

5.4. Complexity analysis

The running time of Algorithm 1 for a graph with n vertices and m edges is $O(mn^2)$, which is $O(n^4)$. First we observe that collecting the initial $a + b$ pebbles in Algorithm 1 requires $O(n)$ for each edge (a total of $O(mn)$) and that the rest of the steps may be charged to $O(m)$ invocations of Algorithm 2.

The running time of Algorithm 2 is $O(n^2)$. This is because each of the $O(n)$ edges in the configuration is enqueued at most once in the main loop, and each edge that is enqueued triggers a basic pebble game search requiring $O(n)$ steps by [11], after first copying a configuration of size $O(n)$.

By way of comparison, a direct application of Knuth's algorithm leads to a more expensive running time. In this approach, one might build the bipartite graph explicitly and use the basic pebble game to test each possible edge. The graph Γ_{H+e} has $O(n^2)$ edges, and each check would require an $O(n^2)$ -time run of the basic pebble game; this would result in a total of running time of $O(mn^4) = O(n^6)$.

5.5. Finding components

Within an $[a, b]$ -sparse graph, an *induced $[a, b]$ -component* is a vertex-maximal $[a, b]$ -block. It is straightforward to adapt Algorithm 1 to maintain and detect induced $[a, b]$ -components, as in the (k, ℓ) -pebble game algorithm with components described in [11]. The running time would remain $O(n^4)$.

Note that any edge with vertices contained in an induced $[a, b]$ -component is dependent and will be rejected by this adapted pebble game in $O(1)$ time. However, an edge may be dependent without being contained in an induced

$[a, b]$ -component, as the circuits in Figure 10 demonstrate. Therefore, *unlike the (k, ℓ) -sparsity case*, we do not save a factor in the running time by maintaining induced $[a, b]$ -components.

5.6. Detecting factor graphs

We now describe algorithms for detecting factor graphs, useful in expressing the pure condition. We begin by detecting factor graphs in a (k, k) -graph before turning to $[a, b]$ -graphs.

5.6.1. The k -factor graphs algorithm.

Given a (k, k) -graph, Algorithm 3 finds the factor graphs associated to the irreducible factors of its pure condition. The basic intuition is that the algorithm detects minimal rigid subgraphs, which are associated to irreducible factors, contracts them (into a vertex representing a rigid body) and recurses. To show

Algorithm 3 The k -factor graphs algorithm.

Input: A (k, k) -graph $G = (V, E)$.

Output: The factor graphs of the irreducible factors of C_G .

Method:

1. Initialize $\mathcal{P} = \emptyset$ and $H = G$.
 2. Play the $(k, k + 1)$ -pebble game on G to find a maximal $(k, k + 1)$ -sparse graph G' .
 3. For every edge e that is rejected (there is at least one):
 - (a) Use the $(k, k + 1)$ -pebble game to detect the fundamental $(k, k + 1)$ -circuit G_e of e in G' .
 - (b) Set $\mathcal{P} = \mathcal{P} + G_e$; set $H = H/G_e$.
 4. If H is not a single vertex:
 - (a) Recursively use the **k -factor graphs algorithm** on H to obtain factor graphs \mathcal{P}' .
 - (b) Set $\mathcal{P} = \mathcal{P} \cup \mathcal{P}'$.
 5. Output \mathcal{P} .
-

correctness, we need to check that every factor graph we find is *irreducible* and *proper*. Properness comes from Theorem 6. Irreducibility of the pure condition of a (k, k) -graph is characterized by White and Whiteley [8, pg. 27]: the pure condition of a graph is irreducible if and only if the graph contains no proper block. The graph contains no proper block if and only if, for every proper subgraph with n' vertices and m' edges, $m' < kn' - k$ (i.e., strict inequality holds on proper subgraphs). Since we are considering a (k, k) -graph with all proper subgraphs $(k, k + 1)$ sparse, this holds precisely when the graph is a $(k, k + 1)$ -circuit.

5.6.2. The $[a, b]$ -factor graphs algorithm.

As shown in Section 4, the factors of an $[a, b]$ -graph have a more complicated combinatorial structure than those of (k, k) -graphs. Therefore, Algorithm 4

adapts the k -factor graphs algorithm to rely on a subroutine (Algorithm 5) that detects the additional types of factors, both proper and improper. These algorithms intuitively follow the same process of detecting rigid components and contracting them; if a contextually rigid component is detected, it is handled in Step 3c of Algorithm 5.

Algorithm 4 The $[a, b]$ -factor graphs algorithm.

Input: an $[a, b]$ -graph $G = (V, E = R \sqcup B)$, with a set of red edges R and a set of black edges B .

Output: Proper (irreducible) and improper factor graphs of G that together provide a factorization of G .

Method:

1. Initialize $\mathcal{P} = \emptyset$; $\mathcal{I} = \emptyset$; $H = G$; set $k = a + b$.
 2. Play the $(k, k + 1)$ -pebble game on G to find a maximal $(k, k + 1)$ -sparse graph G' .
 3. For every edge e that is rejected (there is at least one):
 - (a) Use the $(k, k + 1)$ -pebble game to detect the fundamental $(k, k + 1)$ -circuit G_e of e in G' .
 - (b) Use the $[a, b]$ -**red-factor graphs algorithm** on G_e to obtain sets of factor graphs \mathcal{P}_e and \mathcal{I}_e .
 - (c) Set $\mathcal{P} = \mathcal{P} \cup \mathcal{P}_e$ and $\mathcal{I} = \mathcal{I} \cup \mathcal{I}_e$; set $H = H / G_e$.
 4. If H is not a single vertex:
 - (a) Recursively use the $[a, b]$ -**factor graphs algorithm** on H to obtain sets of factor graphs \mathcal{P}' and \mathcal{I}' .
 - (b) Set $\mathcal{P} = \mathcal{P} \cup \mathcal{P}'$ and $\mathcal{I} = \mathcal{I} \cup \mathcal{I}'$.
 5. Output \mathcal{P} and \mathcal{I} .
-

We provide an overview of how the $[a, b]$ -factor graphs algorithm performs on a $[1, 2]$ -graph with only proper factors in Figure 11 and on a $[1, 1]$ -graph with one improper factor in Figure 12. A more comprehensive trace of the algorithm is given in on a $[1, 1]$ -graph in Figure 14.

We first prove correctness of Algorithm 5.

Claim 5.4. *Algorithm 5 returns only factor graphs; the proper factor graphs are irreducible.*

Proof. The calls to the a -factor graphs algorithm and b -factor graphs algorithm produce irreducible proper factor graphs by the correctness of Algorithm 3. In Step 3.(c)iii we have an $[a, b]$ -fan obtained from a pebble game configuration certifying (a, a) -sparsity of the aqua partition and (b, b) -sparsity of the tan partition. Via sparsity, we also know that there exists an $[a, b]$ -tree decomposition that gives rise to this $[a, b]$ -fan if we direct all edges towards the tie-down. Therefore, by Theorem 8 we know that G' is an $[a, b]$ -graph.

Also by Theorem 8, $H' = H / J$ is a (red) (a, a) -block. Thus, after contracting and recursively calling Algorithm 4, there is exactly one factor graph H'

Algorithm 5 The $[a, b]$ -red-factor graphs algorithm.

Input: An $[a, b]$ -bi-colored graph $G = (V, E = R \sqcup B)$, with a set of red edges R and a set of black edges B , that contains no proper $(a + b, a + b)$ -components.

Output: Proper (irreducible) and improper factor graphs of G that together provide a factorization of G .

Method:

1. Play the (a, a) -pebble game on (V, R) and detect red (a, a) -components.
 2. If no (a, a) -components of (V, R) were found, output $\{G\}$.
 3. Otherwise, let H_1, \dots, H_t be the red (a, a) -components.
 - (a) For each graph $(V(H_i), E(V(H_i)) \cap B)$, play the (b, b) -pebble game to detect (b, b) -components.
 - (b) If no (b, b) -components are found, use the **a -factor graphs algorithm** on each H_i to obtain a set of proper factor graphs \mathcal{P} that are the a -factor graphs of the H_i . Then return \mathcal{P} and $\mathcal{I} = \{(V, E \setminus \{E(V(H_i)) : i \in [t]\})\}$.
 - (c) Otherwise, there is a (b, b) -component J in the vertex span of some component H_i . Set $H = H_i$.
 - i. Use the **a -factor graphs algorithm** on H to obtain a set of factor graphs \mathcal{P}_H .
 - ii. Use the **b -factor graphs algorithm** on J to obtain a set of factor graphs \mathcal{P}_J .
 - iii. Use the $[a, b]$ -pebble game to find an $[a, b]$ -fan of G and collect the remaining k pebbles on a vertex in $V(J)$. Delete every edge of H with its tail in $V(J)$. Contract $V(J)$ into a single vertex to get a graph G' .
 - iv. Use the **$[a, b]$ -factor graphs algorithm** on G' to get a set of factor graphs \mathcal{P}' and \mathcal{I}' .
 - v. Find the factor graph F_H in \mathcal{P}' that contains an edge of H .
 - vi. Return $\mathcal{P}_H \cup \mathcal{P}_J \cup (\mathcal{P}' \setminus \{F_H\})$ and \mathcal{I}' .
-

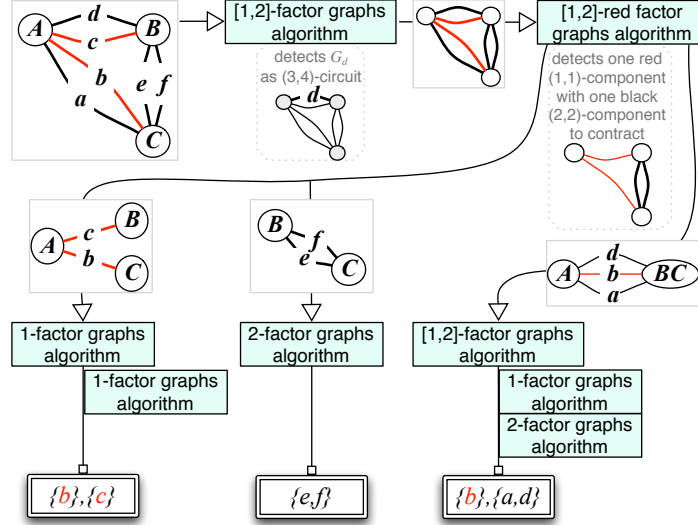


Figure 11: Algorithm 4 finds the proper factor graphs of the $[1, 2]$ -graph underlying Figure 2: $\{\{e, f\}, \{a, d\}, \{b\}, \{c\}\}$; there are no improper factor graphs. The pure condition is $\pm[ef]_{(1,2)}[ad]_{(1,2)}[b]_{(3)}[c]_{(3)}$. A bracket subscripted by ordered tuple T denotes the determinant of the $|T| \times |T|$ matrix with coordinates specified by T .

containing an edge from H , so Step 3(c)v is well-defined. Finally, removing the factor graph $F_H = H'$ from the set of returned factor graphs completes the algorithm's correctness. \square

This, along with Theorem 6, allows us to conclude correctness of our main Algorithm 4:

Claim 5.5. *Algorithm 4 returns only factor graphs, and the proper factor graphs are irreducible.*

We do not know if the improper factor graphs are irreducible, since we do not have a nice representation for them.

Example 5.6 (Example 3.2, continued for the last time). In the (k, k) -setting, if an irreducible factor of P_G is zero, we may identify a (k, k) -subgraph of G that is in a non-generic position, and there is a dependence relation on the rows of the submatrix corresponding to this subgraph.

In our example, setting each factor equal to zero implies the existence of a dependence among the rows of the rigidity matrix of G , but there is an important distinction between the supports of these dependence relations. If $(a_1b_2 - a_2b_1) = 0$ we are guaranteed to get a dependence supported on the first two rows of the rigidity matrix (which contain a and b). However, if $(c_3d_4 - c_4d_3) = 0$, the associated linear dependence *must* involve all four rows

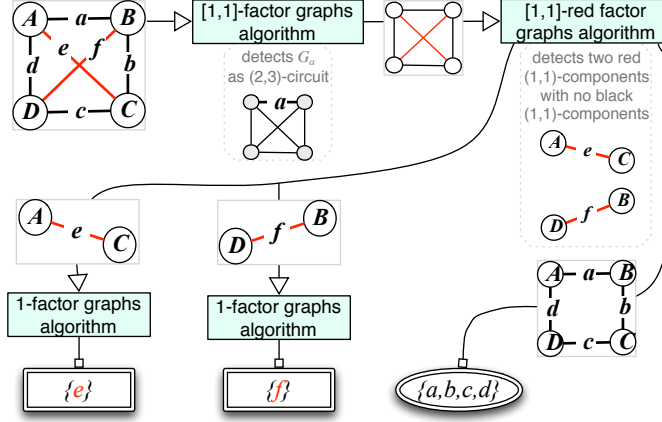


Figure 12: Algorithm 4 on a $[1, 1]$ -graph finds proper factor graphs $\{\{e\}, \{f\}\}$ and an improper factor graph $\{\{a, b, c, d\}\}$. The pure condition is $[e]_{(1)}[f]_{(1)}(a_2b_1c_1d_1 - a_1b_2c_1d_1 - a_1b_1c_2d_1 + a_1b_1c_1d_2) = e_1f_1(a_2b_1c_1d_1 - a_1b_2c_1d_1 - a_1b_1c_2d_1 + a_1b_1c_1d_2)$. A bracket subscripted by ordered tuple T denotes the determinant of the $|T| \times |T|$ matrix with coordinates specified by T .

of the rigidity matrix. This is because there are no conditions on c_1, c_2, d_1 , and d_2 implied by $(c_3d_4 - c_4d_3) = 0$.

What this example is showing is that the rigidity matrix may drop rank because a polynomial supported on a subset of edges vanishes, yet the corresponding dependence in the rigidity matrix may be supported on a set of rows indexed by a larger subset of edges. This phenomenon complicates the correspondence between the combinatorics of G as an $[a, b]$ -graph and factors of P_G .

□

Question 11. *Are all the factor graphs found by Algorithm 4 irreducible?*

6. A case study

In this section we show how a geometric interpretation of the vanishing of the pure condition can be used to predict special positions of the 2D body-and-cad framework consisting of 3 bodies, 2 bars, and 2 line-line coincidence constraints depicted in Figure 2.

The associated primitive cad graph, in which an edge corresponds to a linear constraint, is given in Figure 13(a). In this graph, each line-line coincidence is represented by a red edge, corresponding to a line-line parallel constraint (which restricts only angular motion), and a black edge corresponding to a point-line coincidence constraint (which restricts one translational degree of freedom). Each bar eliminates 1 degree of freedom and is represented by a black edge.

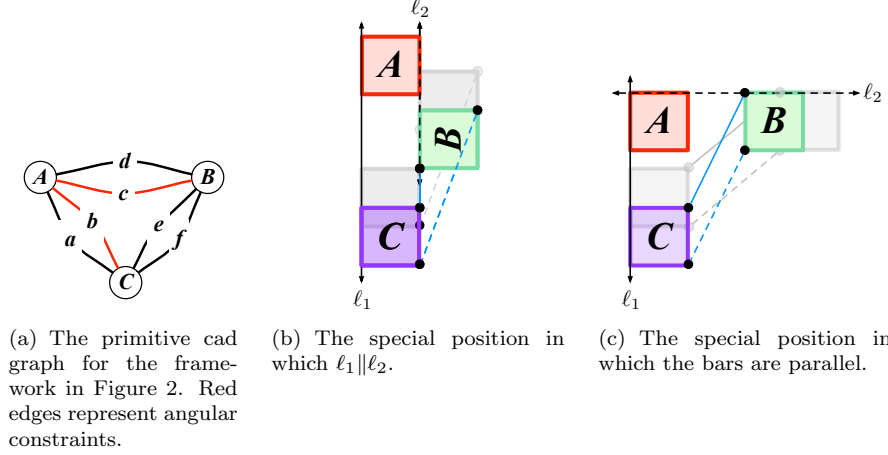


Figure 13: A 2D body-and-cad example on 3 bodies; we assume that body C is tied down.

We will realize this framework in the projective plane \mathbb{P}^2 , which allows us to unify the treatment of rotations and translations if we view an infinitesimal translation as a rotation about a point on the line at infinity. (See [8] and [17] for a detailed introduction to this point of view.) The framework will lie in the affine piece of \mathbb{P}^2 with coordinates $[x : y : 1]$. From this point of view, the line at infinity is $[x : y : 0]$ and parallel lines in the $[x : y : 1]$ -plane meet at a point on the line at infinity corresponding to their slope.

A 2D infinitesimal rigid motion can be represented by a point in $(\mathbb{P}^2)^*$ which is dual to the space in which we embed the framework, and a rotation is represented by a point whose first two coordinates are zero. Note that the point $[0 : 0 : 1] \in (\mathbb{P}^2)^*$ is dual to the line at infinity in our original \mathbb{P}^2 .

If we tie down body C and consider the underlying $(3, 3)$ -graph, the pure condition is the bracket polynomial $[abc][def] - [abd][cef]$. Since the edges labeled b and c correspond to angular constraints, and their last two coordinates are zero, the bracket $[abc]$ evaluates to zero. Therefore, in this case the pure condition is a bracket monomial, $[abd][cef]$, which vanishes when either factor vanishes. Note that the brackets $[abd]$ and $[cef]$ represent reducible polynomials in the coordinates of a, \dots, f . In fact, $[abd] = b_3(a_1d_2 - a_2d_1)$, and $[cef] = c_3(e_1f_2 - e_2f_1)$. Therefore, C_G has four irreducible factors. Compare to the output of Algorithm 4 in Figure 11.

The vanishing of each bracket factor has a geometric interpretation that is obscured in the full polynomial form. The bracket $[abd]$ vanishes when the three points a, b , and d are collinear in $(\mathbb{P}^2)^*$. This means that the lines dual to these three points meet at a point in \mathbb{P}^2 . Since the line dual to b is the line at infinity, this means that the lines dual to a and d meet at a point on the line at infinity. Consequently, these two lines are parallel. In terms of our original geometric constraints, this shows that if lines ℓ_1 and ℓ_2 are parallel, then the body-and-cad

framework is in a special position, and the framework admits an internal motion as depicted in Figure 13(b). Similarly, the bracket $[cef]$ vanishes when the lines dual to e and f are parallel in \mathbb{P}^2 , which is shown in Figure 13(c). Thus, this analysis of the factors of the pure condition associated to the design in Figure 3(a) leads to the useful feedback that “these two lines being parallel cause a dependency,” prompting the problem of automating such an analysis generally, which will require factoring in the *Grassmann-Cayley algebra* when the pure condition is not just a product of brackets.

7. Conclusions

The approach presented in this paper is part of a larger research path to provide computational tools that will give users information about dependencies present in CAD structures in terms of the original geometric constraint system. A prototype of Algorithm 1 has been implemented, with a long-term goal to see the pebble game and factor algorithms incorporated into commercial CAD software packages. By analyzing the pure condition, we can detect special positions of a generically minimally rigid body-and-cad structure. However, since C_G vanishes when $G(\mathbf{p})$ is *infinitesimally* flexible, special positions that we find may not be truly flexible. These positions may still be of interest to a CAD user, as an infinitesimally flexible framework carries an internal stress, indicative of structural weaknesses. Moreover, we may be able to combine conditions implying a special position to create degenerate embeddings with true motions. We conclude with a brief discussion of open questions that arise as we move toward further development of our approach.

Algorithm 4 returns factor graphs of the pure condition of an $[a, b]$ -graph, but it remains open as to whether these factors are irreducible or not. When $b = 0$, the results of White and Whiteley [8] show that irreducible factors of C_G correspond to circuits in G ; this correspondence implies that Algorithm 3 produces irreducible factors for body-and-bar graphs. A better understanding of circuits and stresses would allow us to similarly conclude that the factors identified by Algorithm 4.

We were able to carry out an analysis in the case study of Section 6 where the pure condition was just a product of brackets, and its vanishing was implied by either making two bars parallel or two lines parallel. More generally, a geometric interpretation of the vanishing of a more complicated non-monomial bracket polynomial may be possible via the process of Cayley factorization, which takes as input a polynomial written in terms of brackets of vectors and outputs an expression in terms of meets and joins in the Grassmann-Cayley algebra of those points if such an expression exists. There is a Cayley factorization algorithm due to White [25, 26], and it would be interesting to see if it could be modified (and sped up) if the input bracket polynomial is known to be a pure condition.

Even when a Cayley factorization does exist, it may be nontrivial to extract geometric information about the original framework from it. One issue that adds complexity in general is that a single *cad* constraint may impose multiple linear constraints, so conditions may need to be expressed in terms of sets of

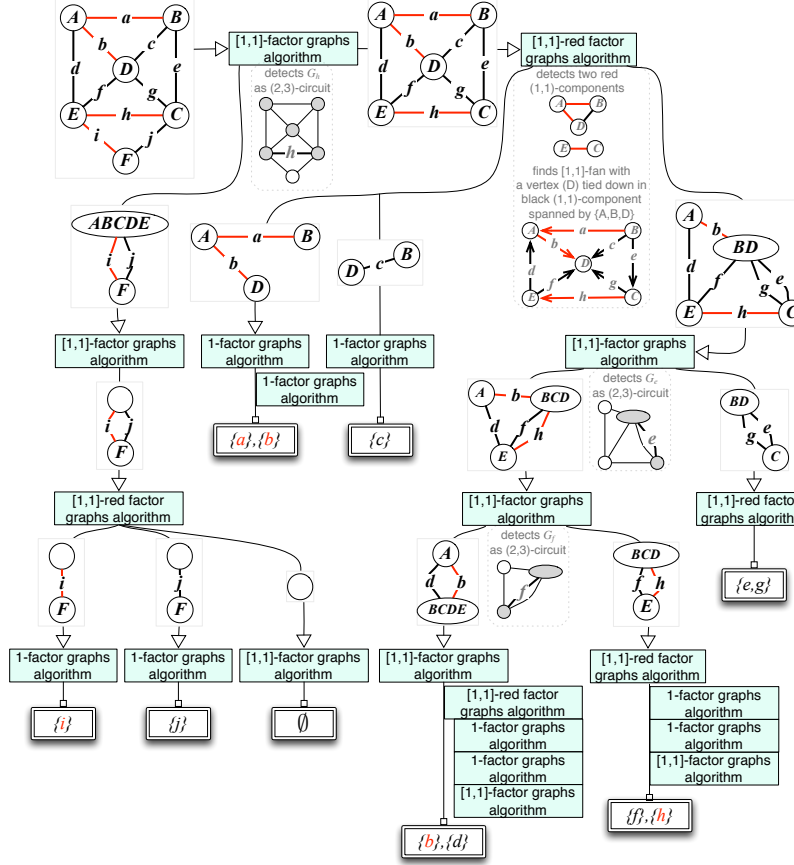


Figure 14: Algorithm 4 on a $[1,1]$ -graph detects proper factor graphs: $\{\{a\}, \{b\}, \{c\}, \{i\}, \{j\}, \{f\}, \{h\}, \{d\}\{e, g\}\}$. There are no improper factor graphs. The pure condition is $\pm[a]_{(1)}[b]_{(1)}[c]_{(2)}[i]_{(1)}[j]_{(2)}[f]_{(2)}[h]_{(1)}[d]_{(2)}[eg]_{(1,2)}$.

vectors. Furthermore, in 3D, the vectors in the brackets do not live in a space dual to our realization space (as they do in 2D), complicating translation of the vanishing of the pure condition into the setting of our original constraints.

Finally, the results in this work rely on the combinatorial characterization of [2], which apply to 3D body-and-cad structures *without point-point coincidence constraints*. While a combinatorial characterization that incorporates these constraints remains unknown, 3D body-and-cad frameworks with point-point coincidences share similar properties with presumed barriers to a combinatorial characterization of 3D bar-and-joint frameworks.

Figures and acknowledgements.

Some figures created in SolidWorks 2010 and 2012. We would like to thank Ruimin Cai for implementing some of the algorithms presented here and Josephine Yu for her work in implementing the Cayley factorization algorithm at the Macaulay2 workshop (Colorado College, Aug. 8-12, 2010; supported by NSF Grant No. 0964128 and NSA Grant No. H98230-10-1-0218.) We are grateful for the thoughtful and constructive feedback from anonymous reviewers.

References

- [1] J. Cheng, M. Sitharam, I. Streinu, Nucleation-free 3d rigidity., in: Proceedings of the 21st Canadian Conference of Computational Geometry, 2009, pp. 71–74.
URL <http://dblp.uni-trier.de/db/conf/cccg/cccg2009.html#ChengSS09>
- [2] A. Lee-St.John, J. Sidman, Combinatorics and the rigidity of cad systems, *Computer-Aided Design* 45 (2) (2013) 473–482.
- [3] S.-C. Chou, Mechanical geometry theorem proving, Vol. 41 of Mathematics and its Applications, D. Reidel Publishing Co., Dordrecht, 1988, with a foreword by Larry Vos.
- [4] F. Geiß, F.-O. Schreyer, A family of exceptional Stewart-Gough mechanisms of genus 7, in: Interactions of classical and numerical algebraic geometry, Vol. 496 of Contemp. Math., Amer. Math. Soc., Providence, RI, 2009, pp. 221–234. doi:10.1090/conm/496/09725.
URL <http://dx.doi.org/10.1090/conm/496/09725>
- [5] X.-S. Gao, D. Lei, Q. Liao, G.-F. Zhang, Generalized stewart-gough platforms and their direct kinematics, *IEEE Transactions on Robotics* 21 (2) (2005) 141.
URL <http://geometrie.uibk.ac.at/institutsangehoerige/husty/dld/Quebec.pdf>
- [6] D. Michelucci, S. Foufou, Detecting all dependences in systems of geometric constraints using the witness method, in: F. Botana, T. Recio (Eds.), Automated Deduction in Geometry, 6th International Workshop (ADG 2006), Vol. 4869 of Lecture Notes in Computer Science, Springer, 2007.
- [7] S. J. Gortler, A. D. Healy, D. P. Thurston, Characterizing generic global rigidity, *Amer. J. Math.* 132 (4) (2010) 897–939. doi:10.1353/ajm.0.0132.
URL <http://dx.doi.org/10.1353/ajm.0.0132>
- [8] N. White, W. Whiteley, The algebraic geometry of motions of bar-and-body frameworks, *SIAM J. Algebraic Discrete Methods* 8 (1) (1987) 1–32. doi:10.1137/0608001.
URL <http://dx.doi.org/10.1137/0608001>
- [9] B. Jackson, J. C. Owen, A characterisation of the generic rigidity of 2-dimensional point-line frameworks, Preprint, arXiv:1407.4675 (2014).
URL <http://arxiv.org/abs/1407.4675>
- [10] W. Whiteley, Some matroids from discrete applied geometry, in: J. Bonin, J. G. Oxley, B. Servatius (Eds.), Matroid Theory, Vol. 197 of Contemporary Mathematics, American Mathematical Society, 1996, pp. 171–311.

- [11] A. Lee, I. Streinu, Pebble game algorithms and sparse graphs, *Discrete Math.* 308 (8) (2008) 1425–1437. doi:10.1016/j.disc.2007.07.104.
URL <http://dx.doi.org/10.1016/j.disc.2007.07.104>
- [12] A. Lee, I. Streinu, L. Theran, Finding and maintaining rigid components, in: *Proceedings of the 17th Canadian Conference of Computational Geometry*, Windsor, Ontario, 2005.
URL <http://cccg.cs.uwindsor.ca/papers/72.pdf>
- [13] T.-S. Tay, Rigidity of multigraphs. I. Linking rigid bodies in n -space, *J. Combin. Theory Ser. B* 36 (1) (1984) 95–112. doi:10.1016/0095-8956(84)90016-9.
URL [http://dx.doi.org/10.1016/0095-8956\(84\)90016-9](http://dx.doi.org/10.1016/0095-8956(84)90016-9)
- [14] G. Laman, On graphs and rigidity of plane skeletal structures, *J. Engrg. Math.* 4 (1970) 331–340.
- [15] M. Sitharam, Y. Zhou, A tractable, approximate characterization of combinatorial rigidity in 3d, in: *5th Automated Deduction in Geometry (ADG)*, 2004.
- [16] D. E. Knuth, Matroid partitioning., Tech. rep., Stanford, CA, USA (1973).
- [17] K. Haller, A. Lee-St.John, M. Sitharam, I. Streinu, N. White, Body-and-cad geometric constraint systems, *Computational Geometry: Theory and Applications* 45 (8) (2012) 385–405.
- [18] W. T. Tutte, On the problem of decomposing a graph into n connected factors, *J. London Math. Soc.* 36 (1961) 221–230.
- [19] C. S. J. A. Nash-Williams, Edge-disjoint spanning trees of finite graphs, *J. London Math. Soc.* 36 (1961) 445–450.
- [20] T. Brylawski, Constructions, in: *Theory of matroids*, Vol. 26 of *Encyclopedia Math. Appl.*, Cambridge Univ. Press, Cambridge, 1986, pp. 127–223. doi:10.1017/CB09780511629563.010.
URL <http://dx.doi.org/10.1017/CB09780511629563.010>
- [21] W. Whiteley, The union of matroids and the rigidity of frameworks, *SIAM J. Discrete Math.* 1 (2) (1988) 237–255. doi:10.1137/0401025.
URL <http://dx.doi.org/10.1137/0401025>
- [22] I. Streinu, L. Theran, Sparsity-certifying graph decompositions, *Graphs and Combinatorics* 25 (2009) 219–238. doi:10.1007/s00373-008-0834-4.
- [23] A. Schrijver, Combinatorial optimization. Polyhedra and efficiency. Vol. B, Vol. 24 of *Algorithms and Combinatorics*, Springer-Verlag, Berlin, 2003, matroids, trees, stable sets, Chapters 39–69.

- [24] M. Berardi, B. Heeringa, J. Malestein, L. Theran, Rigid components in fixed-lattice and cone frameworks, in: Proceedings of the 23rd Annual Canadian Conference on Computational Geometry (CCCG), 2011.
URL <http://arxiv.org/abs/1105.3234>
- [25] N. L. White, Multilinear Cayley factorization, J. Symbolic Comput. 11 (5-6) (1991) 421–438, invariant-theoretic algorithms in geometry (Minneapolis, MN, 1987). doi:10.1016/S0747-7171(08)80113-7.
URL [http://dx.doi.org/10.1016/S0747-7171\(08\)80113-7](http://dx.doi.org/10.1016/S0747-7171(08)80113-7)
- [26] B. Sturmfels, Algorithms in invariant theory, 2nd Edition, Texts and Monographs in Symbolic Computation, SpringerWienNewYork, Vienna, 2008.